JOURNAL OF GEOPHYSICAL RESEARCH, VOL. 114, C04010, doi:10.1029/2008JC005105, 2009

Response of lower trophic level production to long-term climate change in the southeastern Bering Sea

Meibing Jin,[1] Clara Deal,[1] Jia Wang,[2] and C. Peter McRoy[1]

Received 3 September 2008; revised 5 February 2009; accepted 16 February 2009; published 25 April 2009.

[1] The Bering Sea ecosystem has undergone profound changes in response to climate regime shifts in the past decades. Here, lower trophic level production is assessed with a vertically one-dimensional (1-D) coupled ice-ocean ecosystem model, which was applied to data collected by a National Oceanic and Atmospheric Administration (NOAA)/Pacific Marine Environmental Laboratory (PMEL) mooring from 1995 to 2005. The physical model is forced by sea surface winds, heat and salt fluxes, tides, and sea ice. The biological model includes coupled pelagic and ice algae components. Model results are validated with daily mooring temperature, fluorometer, and daily Sea-viewing Wide Field-of-view Sensor (SeaWiFS) chlorophyll data. Two distinct ocean conditions and phytoplankton bloom patterns are related to the Pacific Decadal Oscillation (PDO) Index regimes: warmer temperature and later warm-water phytoplankton species bloom in PDO > 1 year; colder temperature and earlier cold-water phytoplankton species bloom in PDO < -1 year. Productivity of different phytoplankton species changed dramatically after the 1976 climate shift, but the total annual net primary production (NPP) remained flat over the past four decades under similar nutrient regulation. Climate shift also affected the vertical distribution of lower trophic level production and energy flow to the upper ocean pelagic ecosystem or the benthic community. A long-term PDO regime shift occurred in 1976, and a short-term PDO reversal occurred in 1998. Phytoplankton biomass responded promptly to both short- and long-term climate changes. Zooplankton biomass responded more to the long-term than to the short-term climate shift. The model results captured observed trends of zooplankton abundance changes from the 1990s to 2004.

Citation: Jin, M., C. Deal, J. Wang, and C. P. McRoy (2009), Response of lower trophic level production to long-term climate change in the southeastern Bering Sea, *J. Geophys. Res.*, *114*, C04010, doi:10.1029/2008JC005105.

1. Introduction

[2] The Bering Sea shelf is known for its rich marine ecosystem with high primary productivity, abundant fish, and a variety of marine mammals and sea birds. A great deal of progress has been made toward developing an understanding of physical forcing mechanisms and the response of biota over the broad shelf of the Bering Sea. Research programs, such as Process and Resources of the Bering Sea Shelf (PROBES) and the National Oceanic and Atmospheric Administration (NOAA)/Pacific Marine Environmental Laboratory (PMEL) biophysical moorings program have revealed that the marine ecosystem in the Bering Sea responds to climate changes ranging from large-scale climate regime shifts [*Hare and Mantua*, 2000] to small-scale episodic weather events [e.g., *Bond and Overland*, 2005].

[3] In the last century, the northeastern Pacific experienced climate regime shifts in 1926, 1945, 1976, and 1998, as indicated by persistent changes in atmosphere and upper ocean fields, and corresponding shifts of ecosystem structure (abundance and species of zooplankton and fish [*Peterson and Schwing*, 2003]). During the cold years of the early 1970s, a phytoplankton bloom was observed along the ice edge in the early spring; that productivity accounted for a significant proportion of the annual carbon input over the shelf [*Alexander and Niebauer*, 1981]. After the 1976 regime shift from cold to warm, peak primary productivity and phytoplankton biomass usually occurred during the open-water bloom in May or June [*Sambrotto et al.*, 1986; *Whitledge et al.*, 1986], and the timing and magnitude of the spring phytoplankton bloom was found to correlate strongly with sea-ice coverage in winter and spring [*Niebauer et al.*, 1995; *Stabeno et al.*, 1998]. In cases of ice-associated blooms in March and April, the magnitude of the subsequent open-water bloom was reduced in the southeastern Bering Sea middle shelf [*Hunt et al.*, 2002]. Time series data (1995–2001) from a biophysical mooring [*Stabeno et al.*, 2001] in the middle domain of the southeastern shelf support the hypothesis that retreat of the winter

[1] International Arctic Research Center, University of Alaska Fairbanks, Fairbanks, Alaska, USA.
[2] Great Lakes Environmental Research Laboratory, NOAA, Ann Arbor, Michigan, USA.

0148-0227/09/2008JC005105$09.00

sea ice before mid-March (or the failure of ice to be advected into the region) results in an open-water bloom in May or June in relatively warm water (>3°C). Conversely, when ice retreat is delayed until mid-March or later, an ice-associated bloom occurs in cold (<0°C) water in early spring [*Hunt and Stabeno*, 2002].

[4] Besides the interannual atmospheric fluctuations associated with the large-scale Pacific Decadal Oscillation (PDO) [*Zhang et al.*, 1997], the regional Aleutian Low Pressure System [*Niebauer*, 1998], and the Arctic Oscillation (AO) [*Wang and Ikeda*, 2000], rising temperatures and declining sea ice due to greenhouse gas emissions (under global warming) can also have profound impacts on the ecosystem. For example, an ecosystem shift in the northern Bering Sea has been linked to rising global temperatures [*Grebmeier et al.*, 2006].

[5] Observations can directly or indirectly explain some of the primary production changes that were observed in past decades in response to climate changes. However, systematic studies of the response of each ecosystem component to climate changes are hindered by the large temporal and spatial gaps in available observations and incomplete observations of every ecosystem component. Ecosystem models are useful tools for testing scientific hypotheses; they produce spatially and temporally continuous time series to augment patchy observations. Earlier lower trophic level ecosystem modeling studies of the eastern Bering Sea [e.g., *Eslinger and Iverson*, 2001; *Merico et al.*, 2004; *Jin et al.*, 2006a] investigated the impacts of various physical forcings on pelagic ecosystem communities, but they did not include sea ice or ice algae components, and only covered a short time period (seasonal to less than a decade). *Jin et al.* [2007] first simulated and discussed the mechanism of ice-associated phytoplankton blooms that occurred in the southeastern Bering Sea in 1997 and 1999, and revealed that ice-associated phytoplankton production is not only a significant contributor to annual primary production, but may also affect the subsequent warm-water phytoplankton bloom. This enables us to simulate long-term primary production changes in response to both warm- and cold-climate regimes to elucidate ecosystem response.

[6] In this study, we used a coupled ice-ocean ecosystem model [*Jin et al.*, 2007] to conduct a multidecadal simulation to investigate the long-term variability of the southeastern Bering Sea midshelf ecosystem. The model simulation spans 1960 to 2005, thus including the climate regime shifts in 1976 and 1998 [*Peterson and Schwing*, 2003]. The model results were first validated with mooring and remote-sensing data, and then used to analyze ecosystem responses to short-term and long-term climate changes.

2. Methods and Data

[7] The vertically one-dimensional (1-D) ice-associated ecosystem model [*Jin et al.*, 2007] includes both pelagic and ice-algal components, which were incorporated into the Physical-Ecosystem Model (PhEcoM) [*Wang et al.*, 2003]. The pelagic model is coupled with a 1-D physical model containing a level $2^1/_2$ turbulence model [*Mellor*, 2001]. A tidal forcing term was added to the dynamic equations using tidal current harmonic constants derived from Acoustic Doppler Current Profiler (ADCP) observations [*Jin et al.*, 2006a], enabling the combined effects of wind mixing, tidal mixing, and thermal mixing/stratification to be realistically reproduced. PhEcoM was successfully applied to the Bering Sea to study the effects of variations in the physical environment on the spring phytoplankton bloom [*Jin et al.*, 2006a]. An ice-algal model compartment was added by *Jin et al.* [2006b, 2007]. The model equations and parameters and the history of some improvements were introduced by *Jin et al.* [2006a, 2006b, 2007]. A full set of these updated equations and new improvements will be summarized and discussed in a separate paper. The following improvements of the pelagic model are important to the results and discussion of this study and hence the related equations are listed in Appendix A: (1) mesozooplankton and large zooplankton grazing on microzooplankton; (2) temperature-dependent rate of zooplankton grazing, mortality, and respiration [*Kishi et al.*, 2007].

[8] The sea-ice ecosystem model has four compartments: ice algae (Ai) and three nutrients (nitrate + nitrite, ammonium, silicon: NO_3, NH_4, Si). The water column ecosystem model includes 10 compartments: three phytoplankton (pelagic diatoms, flagellates, and cold-water algae: D, F, and Ai), three zooplankton (copepods, large zooplankton, and microzooplankton: ZS, ZL, ZP), three nutrients (nitrate+nitrite, ammonium, silicon: NO_3, NH_4, Si) and detritus (Det). In the water, ice algae should be considered a subset of the cold-water assemblage. Samples taken at ice-edge stations in the Bering Sea by *Schandelmeier and Alexander* [1981] revealed that centric diatoms and chain-forming pennate diatoms found in the slush-ice samples and some ice core samples are also common components of the water column phytoplankton communities. According to the discussions in *Schandelmeier and Alexander* [1981] (their Table 3), the phytoplankton species in the ice-edge bloom differ from those of open-water blooms in two ways.

[9] 1. Species diversity richness: there are 15 taxa living in sea ice; 13 of them also live in the water column, accounting for 1/3 of the total water column species. These ice-associated species prefer the ice-edge environment, and are generally not present in open-water blooms.

[10] 2. Dominant species: the sea-ice-associated species *Nitzschia* spp., *Chaetoceros* spp., and *Achnanthes* spp. are among the most abundant species in ice-edge blooms. In the water column mode, cold-water algae represent diatoms (regardless of their origin in the water column or in ice) with similar biological parameters that differ from warm-water phytoplankton.

[11] The 1-D model results were compared to the data collected at the NOAA/PMEL mooring site M2 (Figure 1a) in the southeastern Bering Sea. Sea ice usually drifts to this mooring site rather than being locally produced. Thus a stand-alone 1-D sea-ice model is not sufficient to simulate the sea-ice conditions. Sea-ice thickness and concentration from large-scale ice-ocean models often have large errors in this marginal ice zone. Sea-ice concentrations obtained from remote sensing were used to approximate the sea-ice thickness changes in the model as in the work of *Jin et al.* [2007]. Because of its availability, we used the Hadley Center's monthly data set HadISST1 [*Rayner et al.*, 2003] before 1978 and daily Special Sensor Microwave/Imager (SSM/I) data (from the National Snow and Ice Data Center

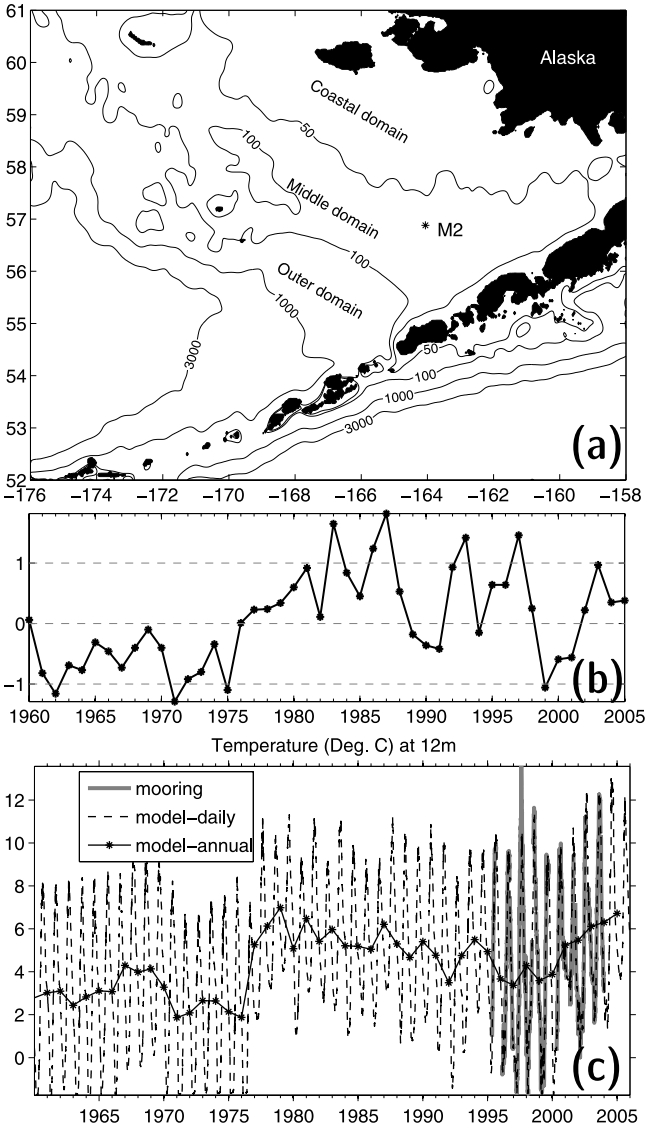

Figure 1. (a) Model domain and NOAA/PMEL mooring M2. (b) Pacific Decadal Oscillation (PDO) Index. (c) Modeled daily and annual mean temperatures at 12 m and comparison with daily mooring data (1997–2005).

[NSIDC], http://nsidc.org/data/seaice) after 1979 to take advantage of higher spatial-temporal resolution. These global data were interpolated from the original 1° grid of HadISST1 and 20 km grid of SSM/I to the mooring site, and temporally to each model time step.

[12] The physical model was forced by tides, National Center for Environmental Protection (NCEP) wind, shortwave radiation, and surface heat and salt fluxes calculated by bulk formulae using NCEP air temperature, precipitation, specific humidity, air pressure, and cloud cover, as described by *Jin et al.* [2006a]. These variables are available from NCEP reanalysis data at 6-hourly time intervals from the Web site at the NOAA-Cooperative Institute for Research in Environmental Studies (CIRES) Climate Diagnostics Center, Boulder, Colorado, USA, http://www.cdc.noaa.gov/.

[13] The water depth, H, is 74 m at the M2 mooring. There are 37 vertical layers with 2 m per layer in both the physical and biological models. The model time step is 2 minutes.

[14] Initial water velocity was set to zero. Since the model run started on 1 January 1960, the initial temperature (T) and salinity (S) were set to be vertically homogeneous based on the mooring data: T = −1.46°C, and S = 31.97.

[15] Initial conditions for the biological model were also set to be vertically homogeneous based on historical measurements. The mooring observations of NO_3 at the M2 site in 2001–2005 were between 8 and 13 mmol m^{-3} in January and up to 15 mmol m^{-3} in late April or early May before the spring bloom (in accordance with *Stabeno et al.* [2006, Figure 7]). NH_4 is nitrified to NO_3 in the model, and this process can increase NO_3 and decrease NH_4 from January to the time of spring bloom. Thus we set NO_3 = 12 mmol N m^{-3} and NH_4 = 2 mmol N m^{-3} in January. Initial conditions for other variables are: D = 0.2 mmol N m^{-3}, F = 0.05 mmol N m^{-3}, ZS = 0.3 mmol N m^{-3}, ZL = 0.01mmol Nm^{-3}, ZM = 0.01 mmol N m^{-3}, Si = 40 mmol Si m^{-3}, and Det = 0 mmol N m^{-3}. The N-based unit can be converted to the chlorophyll-based unit by assuming a carbon: chlorophyll mass ratio of 40 g C (g chl)$^{-1}$ [*Eslinger and Iverson*, 2001] and a C:N molar ratio of 6.625 [*Redfield et al.*, 1963].

[16] The following long-term observational data were used to validate the model and to check model performance in representing seasonal to interannual variability.

[17] 1. Data from the M2 mooring (1995-present): water temperature and salinity were available from multiple vertical layers at 1 m to 62 m depth. The depth and number of layers vary for each variable and equipment deployment period (2 to 3 times per year). Fluorometer observations are generally available at 12 m, 24 m, and 44 m depth with some missing and inaccurate data due to instrument drift.

[18] 2. Daily Sea-viewing Wide Field-of-view Sensor (SeaWiFS) sea surface chlorophyll data (late 1997-present).

3. Results

3.1. Model Validation

[19] This 1-D coupled physical-biological model was validated with both physical and biological observations in two previous studies of the spring bloom that occurred in 2000 [*Jin et al.*, 2006a] and the ice-associated phytoplankton blooms that occurred in 1997 and 1999 [*Jin et al.*, 2007]. The model setting for this study was similar to that by *Jin et al.* [2007], but the model was run for a longer time period: 1960–2007. Here, we further validate the model with more data from 1997–2005 to check the consistency of model performance over the long run, so that the variations in lower trophic level production can be used to study linkage with climate changes.

[20] The simulated temperature at 12 m depth from 1995 to 2005 compared well with the mooring data (Figure 1c). The temperature at 12 m represents the upper mixed layer during spring to early autumn when the water column is stratified, and the entire water column during winter months. The long time series of simulated temperature displayed changes of climate scenarios: a dramatic jump of more than 3°C in 1976/77 accompanied by a PDO Index sign reversal (Figure 1b); several cold winters from 1995 to early 2000; and a steady warming trend from 2000 to 2005. The temperatures at 24 m and 44 m, which represent the

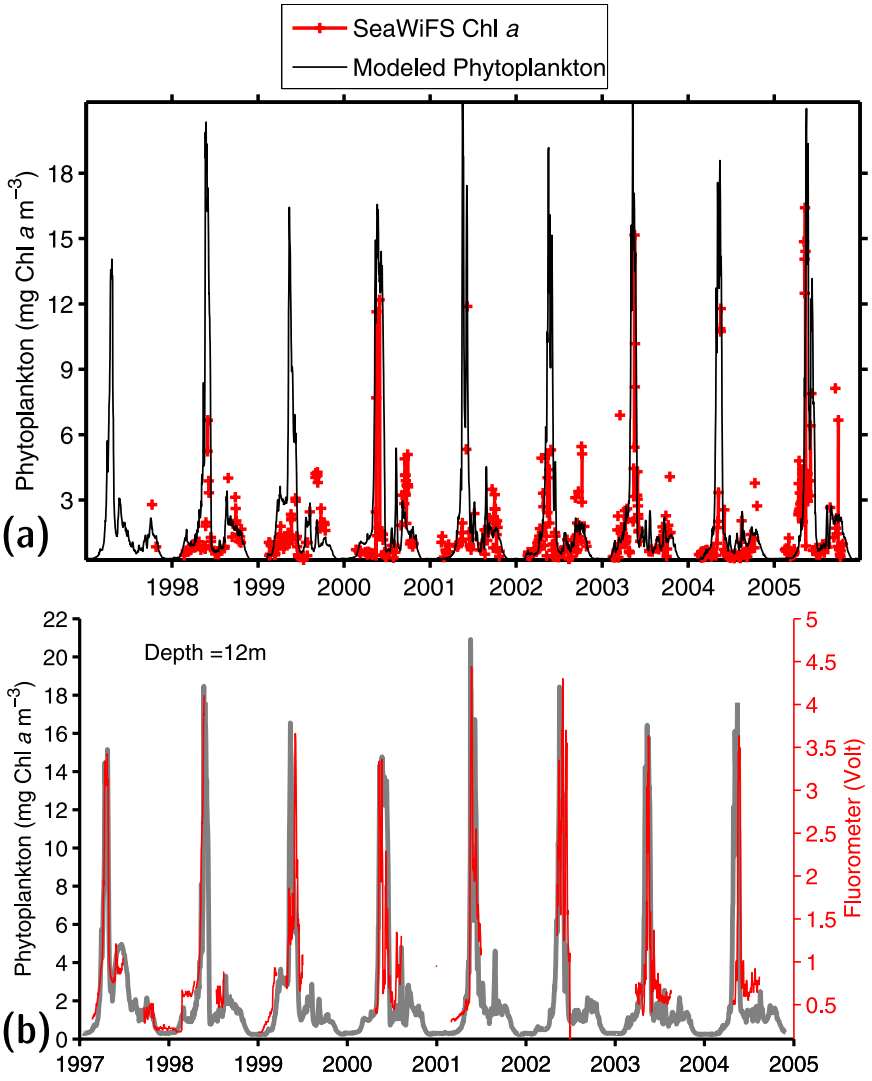

Figure 2. Comparison of modeled phytoplankton with (a) daily Sea-viewing Wide Field-of-view Sensor (SeaWiFS) data at sea surface and (b) mooring fluorescence data at 12 m.

thermohaline and lower mixed layers, also matched the mooring data well (not shown) and displayed similar but smaller climate changes.

[21] The simulated total phytoplankton biomass was compared with daily SeaWiFs and fluorescence measurements at 12 m for 1997–2005 (Figure 2). The model captured the timing, duration, and magnitude of the phytoplankton blooms in most years. Many data points are missing from the daily SeaWiFs record due to cloudy weather, contributing to some of the mismatch of maximum bloom magnitude in 1998, 1999, and 2002. Fluorescence serves as a proxy for phytoplankton biomass and can be converted to units of mg Chl m^{-3} using an appropriate conversion factor, which for this data set has not yet been determined [*Stabeno et al.*, 2001; *Hunt and Stabeno*, 2002]. Thus the fluorometer data are still in units of volts. These have to be corrected for instrumental jumps between deployment periods (generally every three to six months), and a different factor has to be applied to each data set. The factors can be determined simply by visually plotting them on the same time axis to see how different periods of data can be smoothly connected, or numerically by comparing the ending value of the first period with the starting value of the next deployment period. In this way, the long-term series of fluorometer data, although not representing absolute values of Chl-a concentration, are still very useful for validating the timing and relative-magnitude variations of the modeled phytoplankton blooms. During this period, ice-associated phytoplankton blooms, which occurred from late March to early May, were only seen in 1997 and 1999. In the other years, mainly open-water blooms occurred from early May to June in the southeastern shelf region.

3.2. Ocean Conditions and Ecosystem Response in Extreme PDO Years

[22] The ecosystem response to PDO variations is most evident in the differences of physical and biological characteristics between extreme positive and negative PDO years. Here we examined differences between the physical and biological variables averaged in years when the PDO Index was >1 (1983, 1986, 1987, 1993, 1997) and years when the PDO Index was <−1 (1962, 1971, 1975, 1999). The

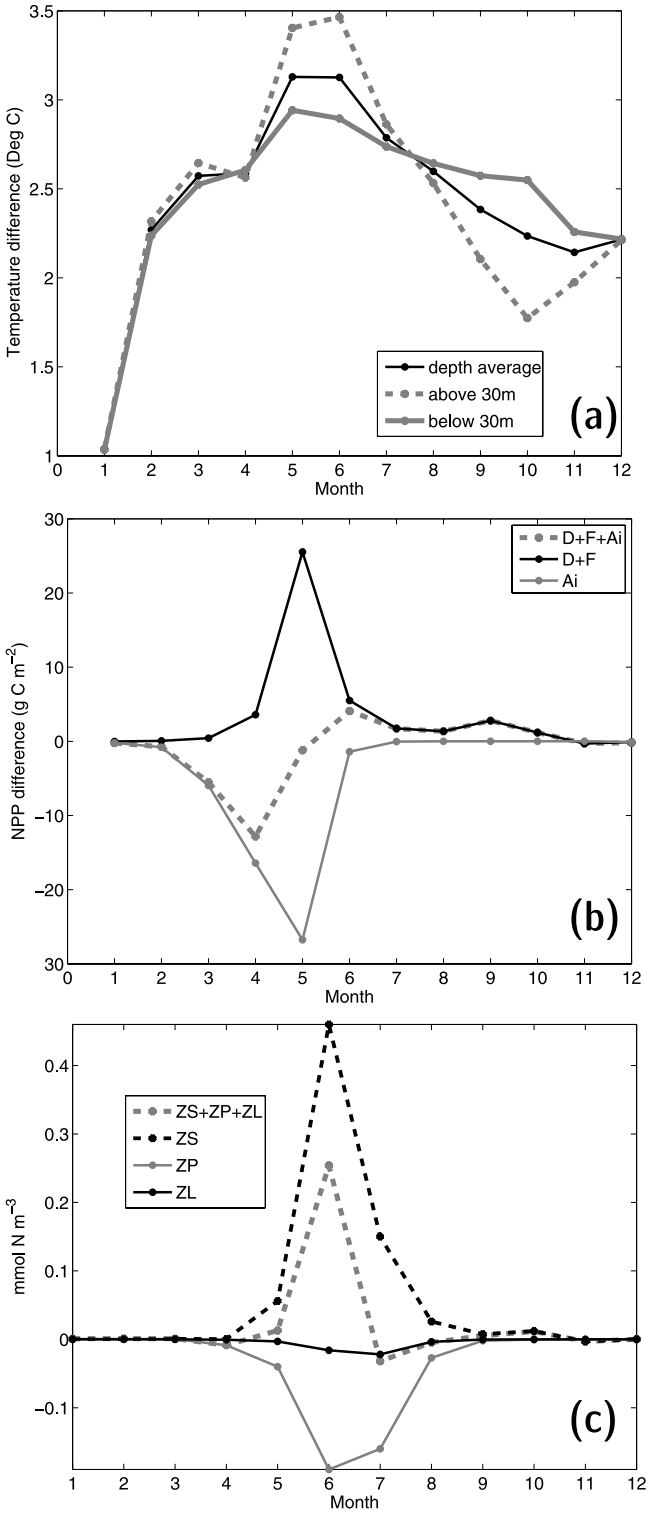

Figure 3. Modeled monthly mean (a) temperature, (b) net primary production (NPP), and (c) zooplankton concentration in years of PDO Index > 1 subtracted by means in years of PDO Index < −1. D, diatoms; F, flagellates; Ai, ice algae; ZP, microzooplankton; ZS, small copepods; ZL, large zooplankton.

temperature difference (Figure 3a) indicated that PDO > 1 years were more than 2°C warmer than PDO < −1 years in most months except January when they were only 1°C warmer. The maximum warming occurred in May to June with more warming at the surface than in the bottom layers, but reversed with more warming at the bottom in September to November.

[23] Since sea ice was present for only a short period in the southeastern Bering Sea, a significant part of the ice-associated primary production occurred in the water column, rather than in the sea ice. Thus this discussion focuses on modeled water column net primary production (NPP; algorithm introduced by *Jin et al.* [2006a]). In extreme negative PDO Index years NPP is higher from March to April, while in extreme positive years NPP is higher from June to October (Figure 3b). The changed production timing was related to the occurrence of two distinct types of phytoplankton blooms under different climate and ocean conditions. In negative PDO Index years, an ice-associated cold-water phytoplankton community predominates with more production in March to May; in negative years a warm-water phytoplankton community (diatoms and flagellates) is most productive from May to October. The modeled zooplankton concentration (Figure 3c) increased most in June and was slightly higher in May and lower in July in positive PDO Index years. Small copepods increased from May to August with the largest population appearing in June, but large zooplankton decreased in June to July and microzooplankton decreased in May to August.

[24] The above results indicate that both physical and biological fields have distinct regimes related to extreme positive and negative PDO indices. How soon and how strongly each biological variable (e.g., phytoplankton groups, zooplankton groups, etc.) responds to a PDO regime shift is hypothesized here to depend on the strength and duration of the index change and ecosystem interactions. Therefore the modeled time series is analyzed in the next section to reveal how the ecosystem components changed as PDO regimes varied over the last four decades.

3.3. Response of Lower Trophic Level Production to Climate Changes

[25] The phytoplankton species composition of the annual NPP (Figure 4a) changed dramatically during the 1976/77 PDO regime shift. Ice-algal production was a significant contribution to the annual NPP during the cold years before 1976, but almost disappeared thereafter, except for several single-year occurrences in the 1990s (1992, 1995, 1997, and 1999). In contrast, total NPP did not show a long-term trend or dramatic change with climate shift, similar to observational findings [*Smith and Vidal*, 1986; *Hunt et al.*, 2002] because the amount of nitrate on the shelf limits new production from new nitrogen [*Dugdale and Goering*, 1967]. The monthly NPP from March to June (Figure 4b) showed a decrease in March and April and an increase in May and June after 1976. This indicates that the peak time of primary production was delayed from April–May to May–June after 1976 in most years when only an open-water bloom occurred.

[26] Changes in phytoplankton biomass caused by climate shifts may affect the ecosystem differently in the surface and bottom layers of the water column. To assess

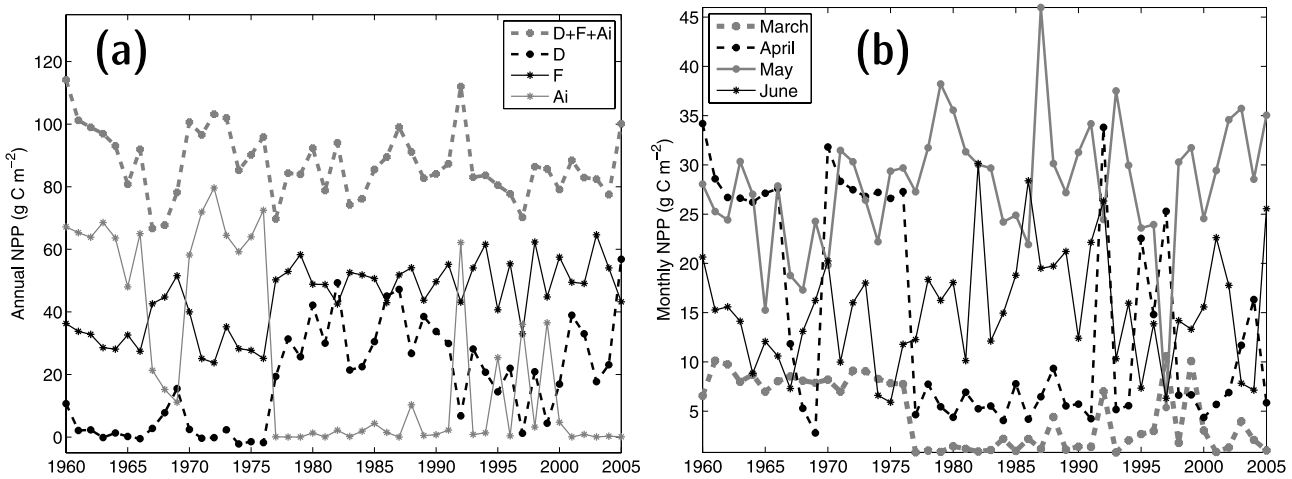

Figure 4. Modeled depth-integrated net primary production (NPP): (a) annual and (b) monthly.

these effects, the time series of simulated phytoplankton concentration above and below 30 m were compared. Note that the mixed-layer depth at the mooring station increases from 10 m (spring) to 30 m (summer), and then deepens to the whole water column in autumn and winter; thus 30 m represents an approximate mean mixed-layer depth and is the most active part of the euphotic zone. In the upper 30 m (Figure 5a) ice algae decreased while diatoms and flagel-

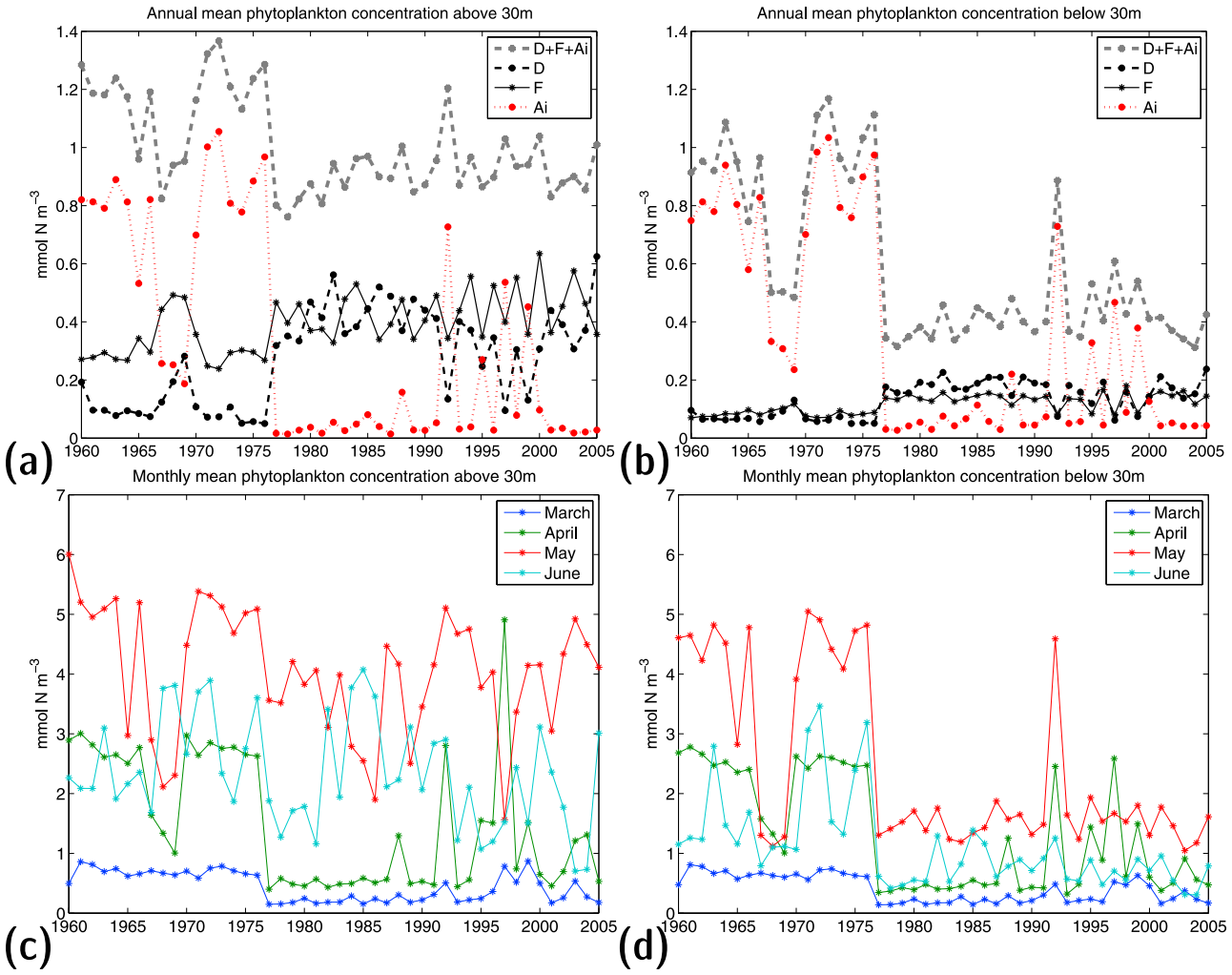

Figure 5. Modeled phytoplankton concentration: (a) annual mean above 30 m, (b) annual mean below 30 m, (c) monthly mean above 30 m, and (d) monthly mean below 30 m.

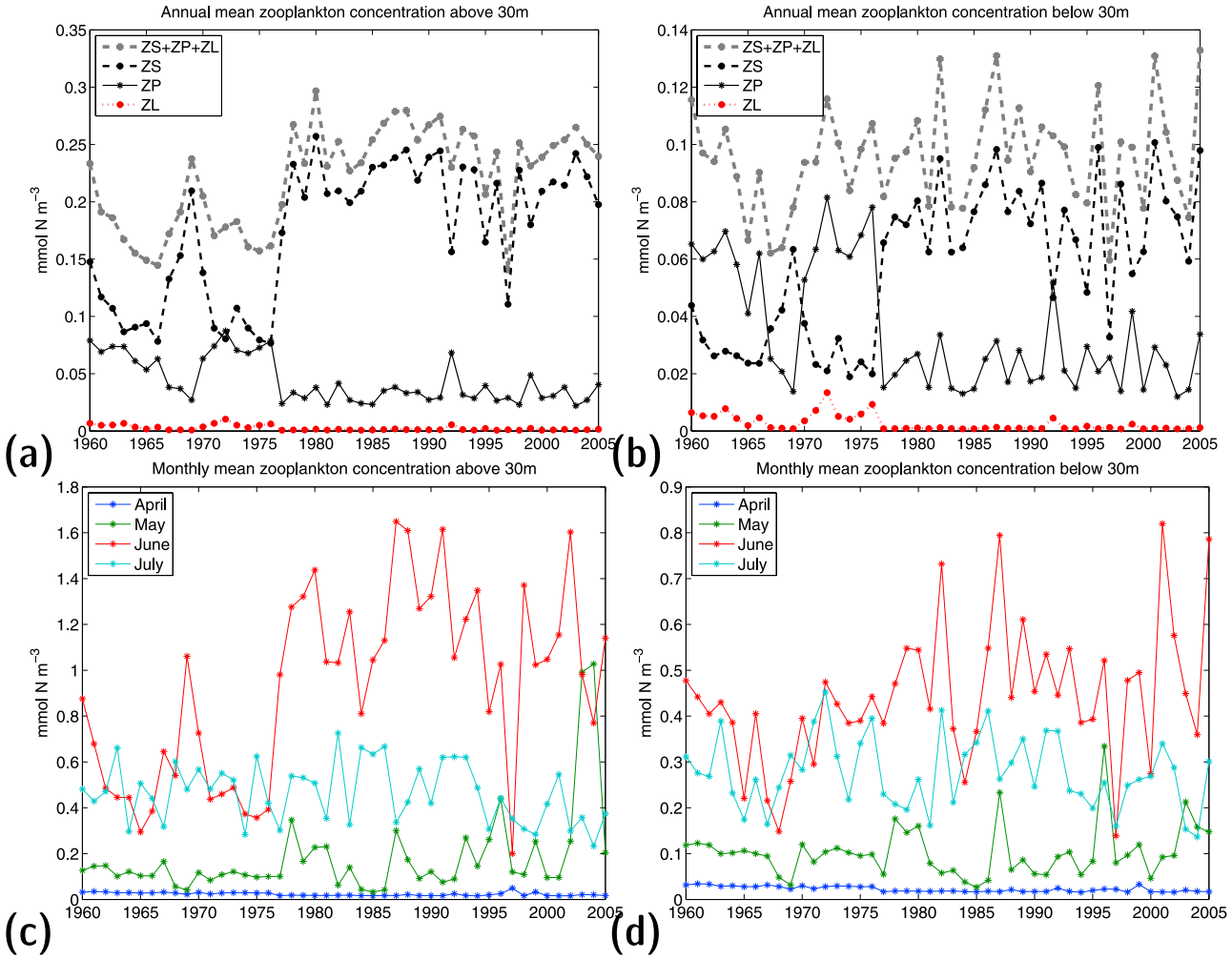

Figure 6. Modeled zooplankton concentration: (a) annual mean above 30 m, (b) annual mean below 30 m, (c) monthly mean above 30 m, and (d) monthly mean below 30 m. ZP, microzooplankton; ZS, small copepods; ZL, large zooplankton.

lates increased after 1976, but there was little change in the total mean phytoplankton concentration. Below 30 m (Figure 5b) ice algae and total phytoplankton concentration decreased after 1976, and little increase was seen in diatoms and flagellates. The decrease of ice-algal production in the bottom layer exceeded that in the surface layer. The decrease of total phytoplankton concentration only occurred in March and April in the upper 30 m (Figure 5c), but in every month from March to June in the bottom layer (Figure 5d). There was an increase of the diatom and flagellate concentrations in the upper 30 m after 1977 (Figure 5a) which maintained the May and June concentration at the same level as before. The increase was not shown in the bottom water (Figure 5b). The different sinking velocity of, and grazing pressure on warm- and cold-water phytoplankton communities were primarily responsible for the different responses in the upper and lower portions of the water column. Ice-associated blooms occurred in 1992, 1995, 1997, and 1999. In other years in the 1980s and 1990s only warm-water blooms occurred; these years appear very different from the other years in Figure 5.

[27] Total annual mean zooplankton concentration in the upper 30 m (Figure 6a) increased after 1976 due to higher grazing rates on the increased phytoplankton production in a later and warmer environment because the zooplankton grazing rate increases with temperature. Increased copepod (ZS) biomass led to a relatively small decrease of microzooplankton (ZP) through grazing. Zooplankton growth depends not only on the phytoplankton concentration, but also on temperature and competition among zooplankton groups. Therefore zooplankton responded differently to the climate shift than did the phytoplankton. In the zooplankton community below 30 m (Figure 6b), copepods also increased and microzooplankton decreased; the changes offset each other and no increase occurred in total zooplankton below 30 m after 1976. The increase of zooplankton mainly occurred in June, but other months showed no evident changes in the upper 30 m (Figure 6c) around 1976. The data from T/S Oshoro Maru surveys conducted in July to early August every year show a decline of zooplankton (summer *C. marshallae* standing stocks) from 1999–2005 and a decline of net-caught zooplankton wet weight from the 1990s to 2005 (as shown in the work of *Hunt et al.* [2008, Figures 17 and 18a]). Model results presented in Figures 6c and 6d showed a slow decline of zooplankton biomass in July after the 1990s both above and below 30 m.

Table 1. Ratio of the Annual Mean Zooplankton Concentration Between May and July to the 10-Year Average From 1995 to 2004

Year	1995	1996	1997	1998	1999	2000	2001	2002	2003	2004
Small copepod	0.66	1.31	0.28	1.15	0.73	0.86	1.27	1.24	1.39	1.11
Large zooplankton	2.17	0.44	0.96	0.37	2.85	0.38	0.64	1.06	0.44	0.69

The modeled zooplankton biomass peaked in June but did not show a decline; there was, however, an increase in May during the same period from the 1990s to 2005 (Figures 6c and 6d). This indicates that the observed decline of total zooplankton in July may be due to a shift of zooplankton production to earlier in the year.

[28] The ratio of the annual modeled mean zooplankton concentration between May and July to the 10-year average from 1995 to 2004 (Table 1) was calculated to compare with the observed zooplankton changes during the same period. The relative variation of modeled small copepod and large zooplankton concentrations reflected the following observed trend of species changes in response to sea ice and climate variations: (1) the middle-shelf abundance of observed large zooplankton (*Calanus marshallae*) in May of 1995 to 1999 was greatest in 1995, 1997, and 1999, years of the most southerly sea-ice extent [*Baier and Napp*, 2003], and (2) in the summer zooplankton community of the middle shelf large zooplankton decreased while small copepods increased between 1999 and 2004 [*Coyle et al.*, 2008].

[29] In the water column below 30 m (Figure 6d), long-term zooplankton changes in all months from April to July were much less dramatic than changes in phytoplankton (Figure 5d), reflecting the fact that the cold-water phytoplankton that prefer bottom communities are rarely grazed and converted to zooplankton biomass; thus, changes in phytoplankton biomass have little impact on zooplankton biomass. On the other hand, changes of the warm-water phytoplankton that prefer pelagic communities can significantly impact the zooplankton biomass in the upper ocean.

4. Discussion and Conclusion

[30] Significant interannual and decadal variability of lower trophic level ecosystems in the southeastern Bering Sea was simulated using the ice-inclusive PhEcoM. The ice-associated primary production in the southeastern Bering Sea may contribute significantly to annual production depending on the timing of sea-ice presence and the weather conditions during and after ice melt [*Alexander and Niebauer*, 1981; *Jin et al.*, 2007]. These critical physical conditions created two distinct phytoplankton bloom patterns in the southeastern Bering Sea, with dominance of either ice-associated cold-water species or warm-water phytoplankton species. While the total annual primary production is controlled by nutrient supplies and exhibited a flat trend in the last four decades, the two phytoplankton bloom patterns switched in response to the long-term climate regime shift as well as to changes in ice and weather conditions in individual years.

[31] The overall ice-associated phytoplankton production dramatically decreased (disappeared in some years), after the PDO Index shifted from a cold to a warm regime after 1976. The consequences were seen in the production shifts of the dominant phytoplankton and zooplankton groups, and the changes in timing, magnitude, and vertical distribution of both primary production and zooplankton biomass. The zooplankton production is very sensitive to the timing of phytoplankton production; e.g., ice-associated phytoplankton produced in the earlier months and in colder water were less grazed (due to lower temperature), sank faster, and contributed more to the benthic biomass and less to the upper ocean than phytoplankton produced in warmer waters in later months [*Riebesell et al.*, 1991; *Nishi and Tabeta*, 2005].

[32] A prolonged period of cold climate will likely lead to bottom-up control on the ecosystem, while a prolonged period of warm climate favors top-down control as the changing primary production effects cascade from lower to higher trophic levels and vice versa [*Hunt and Stabeno*, 2002; *Hunt et al.*, 2002]. Since only a small portion of the lower trophic level biomass is transferred to higher levels and large predators can swim for long distances, it takes a large (temporal and spatial) scale change of primary production for the cascading effect to cause any discernible fishery change. Ocean conditions that can change the occurrence of ice-associated blooms may be significant enough to impact higher trophic levels. An ice-associated cold-water phytoplankton bloom may affect the primary production dramatically, not only because of its contribution to the annual primary production, but also due to its effects on the timing, magnitude, and duration of the subsequent warm-water bloom and vertical energy flows to the benthic biomass or pelagic ecosystem. The southeastern Bering Sea experienced dramatic changes in fish species and abundances after the 1977 PDO Index reversal. The interannual variability of lower trophic production increased around the time of the PDO reversal in 1998, but less is known about changes to the fisheries during the short-lived switching between cold and warm years in the late 1990s.

[33] The effects of natural climate regime shifts, coupled with a long-term gradual warming trend, may induce severe changes in primary production in this region. The Bering Sea ecosystem has also shown a northward shift under the warm climate trend [e.g., *Grebmeier et al.*, 2006]. It is both important and challenging to separate the two effects on primary production. Salinity near M2 usually exerts less influence on primary production than does temperature, but salinity is also an important influence on vertical stratification and primary production as discussed for the open-water bloom that occurred in 2000 [*Jin et al.*, 2006a] and the ice-associated blooms that occurred in 1997 and 1999 [*Jin et al.*, 2007].

Appendix A: The Biological Equations

[34] The pelagic ecosystem model is based on the work of *Jin et al.* [2006a] with the addition of an ice-algal compartment and the following: (1) mesozooplankton and large zooplankton grazing on microzooplankton, and (2) temperature-dependent rate of zooplankton grazing, mortality, and

respiration [*Kishi et al.*, 2007]. There are ten compartments in the water column (nine in *Jin et al.* [2006a]): three phytoplankton (diatom, flagellates and ice algae: *D*, *F* and *Ai*), three zooplankton (small copepods, large copepods, and microzooplankton: *ZS*, *ZL*, *ZP*), three nutrients (nitrate + nitrite, ammonium, silicon: NOB_{3B}, NHB_{4B}, *Si*) and detritus (*Det*):

$$\frac{\partial Ai}{\partial t} = Ai\left(G^{Ai} - R^{Ai} - Rg^{Ai}\right) - \Gamma^{AiS}ZS - \Gamma^{AiL}ZL - \Gamma^{AiP}ZP + \frac{\partial\left(W^{Ai}Ai\right)}{\partial z} + \Phi_{Ai} \tag{A1}$$

$$\frac{\partial D}{\partial t} = D\left(G^{D} - R^{D} - Rg^{D}\right) - \Gamma^{DS}ZS - \Gamma^{DL}ZL - \Gamma^{DP}ZP + \frac{\partial(W^{D}D)}{\partial z} + \Phi_{D} \tag{A2}$$

$$\frac{\partial F}{\partial t} = F\left(G^{F} - R^{F} - Rg^{F}\right) - \Gamma^{FS}ZS - \Gamma^{FL}ZL - \Gamma^{FP}ZP + \frac{\partial(W^{F}F)}{\partial z} + \Phi_{F} \tag{A3}$$

$$\frac{\partial ZS}{\partial t} = ZS\left[A^{S}\left(\Gamma^{DS} + \Gamma^{FS} + \Gamma^{AiS} + \Gamma^{PS}\right)\left(1 - Ex^{S}\right) - M^{S}\right] + \Phi_{ZS} \tag{A4}$$

$$\frac{\partial ZL}{\partial t} = ZL\left[A^{L}\left(\Gamma^{DL} + \Gamma^{FL} + \Gamma^{AiL} + \Gamma^{PL}\right)\left(1 - Ex^{L}\right) - M^{L}\right] + \frac{\partial(W^{L}ZL)}{\partial z} + \Phi_{ZL} \tag{A5}$$

$$\frac{\partial ZP}{\partial t} = ZP\left[A^{P}\left(\Gamma^{DP} + \Gamma^{AiP} + \Gamma^{FP}\right)\left(1 - Ex^{P}\right) - M^{P}\right] - \Gamma^{PS}ZS - \Gamma^{PL}ZL + \Phi_{ZP} \tag{A6}$$

$$\frac{\partial NO_3}{\partial t} = -f_{NO3}\left[D\left(G^{D} - R^{D}\right) + F\left(G^{F} - R^{F}\right) + Ai\left(G^{Ai} - R^{Ai}\right)\right] + C_{AtoN}\cdot NH_4 + \Phi_{NO3} \tag{A7}$$

$$\frac{\partial NH_4}{\partial t} = ZS\cdot A^{S}\left(\Gamma^{DS} + \Gamma^{FS} + \Gamma^{AiS} + \Gamma^{PS}\right)Ex^{S} + ZL\cdot A^{L}\left(\Gamma^{DL} + \Gamma^{FL} + \Gamma^{AiL} + \Gamma^{PL}\right)Ex^{L} + ZP\cdot A^{P}\left(\Gamma^{DP} + \Gamma^{FP} + \Gamma^{AiP}\right)Ex^{M} + D\cdot Rg^{D} + F\cdot Rg^{F} + Ai\cdot Rg^{Ai} + Det\cdot Rg^{Det} - \left(1 - f_{NO_3}\right)\left[D\left(G^{D} - R^{D}\right) + F\left(G^{F} - R^{F}\right) + Ai\left(G^{Ai} - R^{Ai}\right)\right] - C_{AtoN}\cdot NH_4 + \Phi_{NH4} \tag{A8}$$

$$\frac{\partial Si}{\partial t} = -\kappa_{Si}\left[D\left(G^{D} - R^{D}\right) + Ai\left(G^{Ai} - R^{Ai}\right)\right] + \Phi_{Si} \tag{A9}$$

$$\frac{\partial Det}{\partial t} = ZS\cdot\left[\left(1 - A^{S}\right)\left(\Gamma^{DS} + \Gamma^{FS} + \Gamma^{AiS} + \Gamma^{PS}\right) + M^{S}\right] + ZL\cdot\left[\left(1 - A^{L}\right)\left(\Gamma^{DL} + \Gamma^{FL} + \Gamma^{AiL} + \Gamma^{PL}\right) + M^{L}\right] + ZP\cdot\left[\left(1 - A^{P}\right)\left(\Gamma^{DP} + \Gamma^{FP} + \Gamma^{AiP}\right) + M^{P}\right] - Det\cdot Rg^{Det} + \frac{\partial(W^{Det}Det)}{\partial z} + \Phi_{Det} \tag{A10}$$

where superscripts *D*, *F*, and *Ai* denote diatoms, flagellates, and ice algae in the water column, and superscripts *S*, *L*, and *P* denote small copepods, large copepods, and microzooplankton. The ratio of phytoplankton growth due to nitrate uptake to growth due to both nitrate and ammonium uptake (f_{NO3}) follows *Eslinger et al.* [2001]. The last term Φ of each equation denotes vertical diffusion. Terms *G*, *R*, and *Rg* are phytoplankton growth rate, respiration rate, and mortality rate, respectively.

$$G^{X} = \mu_0^{X} e^{rT} \times \min\left(N_{frac}, Si_{frac}, I_{frac}\right) \tag{A11a}$$

(for diatoms and flagellates)

$$G^{Ai} = \mu_0^{Ai} e^{T_{freeze} - T} \times \min(N_{frac}, Si_{frac}, I_{frac})\xi \tag{A11b}$$

(for ice algae [*Jin et al.*, 2007])

$$R^{X} = 0.05\mu_0^{X} e^{rT} \tag{A11c}$$

$$Rg^{X} = Rg_0 e^{r_g T} \tag{A11d}$$

[35] The superscript *X* denotes *D*, *F*, or *Ai*. μ_0^X is the maximum phytoplankton growth rate at 0°C. T_{freeze} is the freezing temperature of the sea water. N_{frac}, Si_{frac}, I_{frac} are unitless ratios expressing nitrogen, silicon, and light limitation as defined by *Eslinger et al.* [2001]. Si_{frac} is only used for diatoms. Γ^{XY} denotes the grazing rate of zooplankton *Y* on phytoplankton or microzooplankton *X*, formulated as modified Ivlev-type grazing [*Ivlev*, 1945; *Eslinger et al.*, 2001] with temperature-dependent rates:

$$\Gamma^{XY} = \Gamma_{XY}\left(1 - e^{-\lambda_{XY}(X - X_Y)}\right)e^{rT} \tag{A12}$$

[36] The zooplankton grazing rate is also expressed as temperature dependent:

$$M^{Y} = M_0^{Y} e^{rT} \tag{A13}$$

[37] Note the temperature-dependent rate (*r*) in equations (A11) to (A13) is set to 0.0633 Deg^{-1} as in the work of *Kishi et al.* [2007]. Other parameters discussed in the work of *Jin et al.* [2006a, 2006b, 2007] are not repeated here.

[38] The microzooplankton grazing rate ($\Gamma_{XY} = 0.01\ h^{-1} = 0.24\ d^{-1}$ [*Jin et al.*, 2006a]) was set within the range of microzooplankton grazing on phytoplankton cells observed by *Olson and Strom* [2002] in the middle-shelf domain in July 1999. *Strom and Frederickson* [2008, Table 2] lists average microzooplankton grazing rates from the southeastern Bering Sea as 0.26 d^{-1} for June–July 1999 [*Liu et al.*, 2002], 0.29 d^{-1} for July–August 1999 [*Olson and Strom*, 2002], and a "low" average rate of 0.13 d^{-1} in July–August 2004 [*Strom and Fredrickson*, 2008]. Parameteriza-

tion of grazing in the model allows the grazing rate to be decreased if phytoplankton biomass is low.

[39] **Acknowledgments.** We are grateful to Phyllis Stabeno and Sigrid Sallo, PMEL/NOAA, Seattle, Washington, for providing the M2 buoy and mooring data. This study was supported by North Pacific Research Board (NPRB) grant 607 awarded to Jin, Deal, and Wang. The International Arctic Research Center, University of Alaska Fairbanks, supported this study through the JAMSTEC-IARC Research Agreement and NSF ARC-0652838. This is NPRB contribution 194 and NOAA GLERL contribution 1494.

References

Alexander, V., and H. J. Niebauer (1981), Oceanography of the eastern Bering Sea ice-edge zone in spring, *Limnol. Oceanogr.*, *26*(6), 1111–1125.

Baier, C. T., and J. M. Napp (2003), Climate-induced variability in *Calanus marshallae* populations, *J. Plankton Res.*, *25*, 771–782.

Bond, N. A., and J. E. Overland (2005), The importance of episodic weather events to the ecosystem of the Bering Sea shelf, *Fish. Oceanogr.*, *14*(2), 97–111.

Coyle, K. O., A. I. Pinchuk, L. B. Eisner, and J. M. Napp (2008), Zooplankton species composition, abundance and biomass on the eastern Bering Sea shelf during summer: The potential role of water column stability and nutrients in structuring the zooplankton community, *Deep Sea Res., Part II*, *55*, 1775–1791.

Dugdale, R. C., and J. J. Goering (1967), Uptake of new and regenerated forms of nitrogen in primary productivity, *Limnol. Oceanogr.*, *12*, 196–206.

Eslinger, D. L., and R. L. Iverson (2001), The effects of convective and wind-driven mixing on spring phytoplankton dynamics in the southeastern Bering Sea middle shelf domain, *Cont. Shelf Res.*, *21*, 627–650.

Eslinger, D. L., R. T. Cooney, C. P. McRoy, A. Ward, T. Kline, E. P. Simpson, J. Wang, and J. R. Allen (2001), Plankton dynamics: Observed and modeled responses to physical forcing in Prince William Sound, Alaska, *Fish. Oceanogr.*, *10*(suppl. 1), 81–96.

Grebmeier, J. M., J. E. Overland, S. E. Moore, E. V. Farley, E. C. Carmack, L. W. Cooper, K. E. Frey, J. H. Helle, F. A. McLaughlin, and S. L. McNutt (2006), A major ecosystem shift in the northern Bering Sea, *Science*, *311*, 1461–1464, doi:10.1126/science.1121365.

Hare, S. R, and N. J. Mantua (2000), Empirical evidence for North Pacific regime shifts in 1977 and 1989, *Prog. Oceanogr.*, *47*, 103–146.

Hunt, G. L., and P. J. Stabeno (2002), Climate change and the control of energy flow in the southeastern Bering Sea, *Prog. Oceanogr.*, *55*, 5–22.

Hunt, G. L., P. J. Stabeno, G. Walters, E. Sinclair, R. D. Brodeur, J. M. Napp, and N. A. Bond (2002), Climate change and control of the southeastern Bering Sea pelagic ecosystem, *Deep Sea Res., Part II*, *49*, 5821–5853.

Hunt, G. L., P. J. Stabeno, S. Strom, and J. M. Napp (2008), Patterns of spatial and temporal variation in the marine ecosystem of the southeastern Bering Sea, with special reference to the Pribilof Domain, *Deep Sea Res., Part II*, *55*, 1919–1944.

Ivlev, V. S. (1945), The biological productivity of waters, *Usp. Sovern. Biol.*, *19*, 98–102.

Jin, M., C. J. Deal, J. Wang, N. Tanaka, and M. Ikeda (2006a), Vertical mixing effects on the phytoplankton bloom in the southeastern Bering Sea midshelf, *J. Geophys. Res.*, *111*, C03002, doi:10.1029/2005JC002994.

Jin, M., C. J. Deal, J. Wang, K. H. Shin, N. Tanaka, T. E. Whitledge, S. H. Lee, and R. R. Gradinger (2006b), Controls of the landfast ice-ocean ecosystem offshore Barrow, Alaska, *Ann. Glaciol.*, *44*, 63–72.

Jin, M., C. Deal, J. Wang, V. Alexander, R. Gradinger, S. Saitoh, T. Iida, Z. Wan, and P. Stabeno (2007), Ice-associated phytoplankton blooms in the southeastern Bering Sea, *Geophys. Res. Lett.*, *34*, L06612, doi:10.1029/2006GL028849.

Kishi, M. J., et al. (2007), NEMURO—A lower trophic level model for the North Pacific marine ecosystem, *Ecol. Modell.*, *202*, 12–25.

Liu, H., K. Suzuki, and T. Saino (2002), Phytoplankton growth and microzooplankton grazing in the subarctic Pacific Ocean and the Bering Sea during summer 1999, *Deep Sea Res., Part I*, *49*, 363–375.

Mellor, G. L. (2001), One-dimensional, ocean surface layer modeling: A problem and a solution, *J. Phys. Oceanogr.*, *31*, 790–809.

Merico, A., T. Tyrrel, E. J. Lessard, T. Oguz, P. J. Stabeno, S. I. Zeeman, and T. E. Whitledge (2004), Modeling phytoplankton succession on the Bering Sea shelf: Role of climate influences and trophic interactions in generating *Emiliania huxleyi* blooms 1997–2000, *Deep Sea Res., Part I*, *51*, 1803–1826.

Niebauer, H. (1998), Variability in Bering Sea ice cover as affected by a regime shift in the North Pacific in the period 1947–1996, *J. Geophys. Res.*, *103*(C12), 27,717–27,737.

Niebauer, H. J., V. Alexander, and S. M. Henrichs (1995), A time series study of the spring bloom at the Bering Sea ice edge. I: Physical processes, chlorophyll, and nutrient chemistry, *Cont. Shelf Res.*, *15*, 1859–1877.

Nishi, Y., and S. Tabeta (2005), Analysis of the contribution of ice algae to the ice-covered ecosystem in Lake Saroma by means of a coupled ice-ocean ecosystem model, *J. Mar. Syst.*, *55*, 249–270.

Olson, M. B., and S. L. Strom (2002), Phytoplankton growth, microzooplankton herbivory and community structure in the southeast Bering Sea: Insight into the formation and temporal persistence of an *Emiliania huxleyi* bloom, *Deep Sea Res., Part II*, *49*, 5969–5990.

Peterson, W. T., and F. B. Schwing (2003), A new climate regime in northeast Pacific ecosystems, *Geophys. Res. Lett.*, *30*(17), 1896, doi:10.1029/2003GL017528.

Rayner, N. A., D. E. Parker, E. B. Horton, C. K. Folland, L. V. Alexander, D. P. Rowell, E. C. Kent, and A. Kaplan (2003), Global analyses of sea surface temperature, sea ice, and night marine air temperature since the late nineteenth century, *J. Geophys. Res.*, *108*(D14), 4407, doi:10.1029/2002JD002670.

Redfield, A. C., B. H. Ketchum, and F. A. Richards (1963), The influence of organisms on the composition of seawater, in *The Sea*, edited by M. N. Hill, vol. 2, pp. 26–79, Wiley-Interscience, Hoboken, N. J.

Riebesell, U., I. Scholoss, and V. Smetacek (1991), Aggregation of algae released from melting sea ice: Implications for seeding and sedimentation, *Polar Biol.*, *11*, 239–248.

Sambrotto, R. N., H. J. Niebauer, J. J. Goering, and R. L. Iverson (1986), Relationships among vertical mixing, nitrate uptake and phytoplankton growth during the spring bloom in the southeast Bering Sea middle shelf, *Cont. Shelf Res.*, *5*, 161–198.

Schandelmeier, L., and V. Alexander (1981), An analysis of the influence of ice on spring phytoplankton population structure in the southeast Bering Sea, *Limnol. Oceanogr.*, *26*(5), 935–943.

Smith, S. L., and J. Vidal (1986), Variations in the distribution, abundance, and development of copepods in the southeastern Bering Sea in 1980 and 1981, *Cont. Shelf Res.*, *5*(1–2), 215–239.

Stabeno, P. J., J. D. Schumacher, R. F. Davis, and J. M. Napp (1998), Under-ice observations of water column temperature, salinity, and spring phytoplankton dynamics: Eastern Bering Sea shelf, *J. Mar. Res.*, *56*, 239–255.

Stabeno, P. J., A. Bond, B. Kachel, A. Salo, and J. D. Schumacher (2001), On the temporal variability of the physical environment over the southeastern Bering Sea, *Fish. Oceanogr.*, *10*(1), 81–98.

Stabeno, P., J. Napp, and T. Whitledge (2006), Long-term observations on the Bering Sea shelf (2004–2005): Biophysical moorings at sites 2 and 4 as sentinels for ecosystem change, *NPRB Project 410 Final Rep.*, Anchorage, Alaska.

Strom, S. L., and K. A. Fredrickson (2008), Intense stratification leads to phytoplankton nutrient limitation and reduced microzooplankton grazing in the southeastern Bering Sea, *Deep Sea Res., Part II*, *55*, 1761–1774.

Wang, J., and M. Ikeda (2000), Arctic oscillation and Arctic sea-ice oscillation, *Geophys. Res. Lett.*, *27*(9), 1287–1290.

Wang, J., C. Deal, Z. Wan, M. Jin, N. Tanaka, and M. Ikeda (2003), User's guide for a Physical-Ecosystem Model (PhEcoM) in the subpolar and polar oceans, version 1, *IARC-FRSGC Tech. Rep. 03-01*, 75 pp., Int. Arctic Res. Cent., Fairbanks, Alaska.

Whitledge, T. E., W. S. Reeburgh, and J. J. Walsh (1986), Seasonal inorganic nitrogen distributions and dynamics in the southeastern Bering Sea, *Cont. Shelf Res.*, *5*, 109–132.

Zhang, Y., J. M. Wallace, and D. S. Battisti (1997), ENSO-like interdecadal variability: 1900–93, *J. Clim.*, *10*, 1004–1020.

C. Deal, M. Jin, and C. P. McRoy, International Arctic Research Center, University of Alaska Fairbanks, 930 Koyukuk Drive, Fairbanks, AK 99775, USA. (ffjm@uaf.edu)

J. Wang, Great Lakes Environmental Research Laboratory, NOAA, 4840 S. State Road, Ann Arbor, MI 48108, USA.